MH-60 Droop Stop Pounding Identification

Dr. Suresh Moon[1], Daniel Liebschutz[2]

[1]*Chief Engineer, Air Vehicle Engineering,* ***Technical Data Analysis Inc., USA***

[2]*Team Lead Engineer, Rotary Wing Structures,* ***NAVAIR, USA***

Abstract

The design Droop Stop Pounding (DSP) occurrences contribute 52% and GAG cycles contribute 17% of fatigue damage to the spindle fatigue life. Thus to increase the spindle fatigue life it is necessary to properly identify the DSP occurrences in the fleet and use it to compute fatigue damage. DSP is usually caused by maneuvering during Near As Possible (NAP) of earth flying, slope landings, rolling landings, and low g pushovers when the pilot applies significant cyclic and suddenly reduces collective stick position. The low Nz values with associated blade flap deflection is utilized to identify DSP during pushover. Lateral and collective control stick positions and their rates with associated blade flap angles were utilized to identify DSP during slope landings, rolling landings, taxi, taxi turns, rotor start, and stop. DSP recognition logic was programmed and ran through MH-60 data of 58,348 IMD flights with 84,549 rotor hours from 308 rotorcraft to obtain DSP utilization. The wide variation in DSP usage was observed from rotorcraft to rotorcraft. The fleet occurrences of DSP during these maneuvers are significantly lower than design. The impact of DSP on fatigue life of MH-60S spindle was studied with RR recognized DSP occurrences. Individual rotorcraft usage with serial number fatigue tracking will help to increase spindle fatigue life, enhance safety, and reduce cost.

1.0 Introduction

Droop Stop Pounding (DSP) is usually caused by maneuvering during Near As Possible (NAP) of earth flying, slope landings, rolling landings, and low g pushovers when the pilot applies significant cyclic and suddenly reduces collective stick position. The sudden reduction in collective stick position reduces thrust to a very low value or zero. Thus moment created by the horizontal component of thrust about the rotorcraft's center of gravity is zero thereby leading to loss of control between the main rotor and fuselage. The moment due to unbalanced tail rotor thrust, rolls or yaws the fuselage to the right and rotor disc to the left due to cyclic input and the main rotor starts DSP and hits the rotor mast (mast bumping). The excessive forward cyclic during taxing or excessive aft cyclic during rearward taxi with low collective can cause DSP. During a rolling landing the excessive aft cyclic with low collective with all wheels on ground can also cause DSP. During rotor start, RPM increases from 0 to 100%, this leads to an increase in centrifugal force from 0 to 100%. However, within the low rotor RPM range below 70%, the sudden significant change in lateral and collective stick position results

in DSP as there is not enough centrifugal force and vertical shear to keep blade at a constant flap deflection. With rotor shutdown, rotor RPM decreases from 100% to 0%, the centrifugal force decreases from 100% to 0% and vertical shear decreases. Thus low and high rotor blade flapping during low RPM also causes DSP.

DSP induces high amplitude stress on rotor hub components and is the main contributor to shorter fatigue life. Sometimes stresses due to DSP may be beyond design limit stress. Thus, to restrict high and low blade flap motions, flap restrainers and droop stops are incorporated in the rotor hub. The number of DSP occurrences is assumed and fatigue life is computed. Now that an Integrated Mechanical Diagnostics System (IMD) is installed on MH-60 helicopters to record flight parameters and control stick positions, it is necessary to develop a DSP identification algorithm so actual DSP occurrences to which individual rotorcraft are subjected, are counted and utilized to compute component fatigue life. With this approach, component fatigue life can be extended and rotorcraft safety can be insured.

2.0 MH-60 IMD HUMS

The IMD HUMS Airborne Unit (AU) consists of a Main Processor Unit (MPU), an optical tracker, Remote Data Concentrators (RDC), and Cockpit Display Unit (CDU) as shown in Figure 1. The details of the IMD system can be found in Reference 1-3. The RDC is suite of sensors/transducers ranging from 30 to 70 sensors on various airframe structures and components (engine, drive train, rotor components). The processor can receive analog or digital MIL-STD-1553 data bus input. The MPU consists of Primary Processor Unit (PPU) and Vibration Processor Unit (VPU). The MPU samples the data at 10Hz, and stores values at 1Hz. In the event of exceedances, the MPU receives data from the VPU and stores 10 Hz data 15 seconds prior to exceedance event and 15 second after the exceedance event. The MPU sends data to the Data Transfer Unit (DTU), Figure 1. DTU stores data on PCMCIA flash memory. The binary data from PCMCIA card is transferred to ground station for transmission to IMD Severs. The main functions of the IMD HUMS system are: (1) drive train, rotors, and engine vibrations diagnostics, (2) onboard rotor track and balance, (3) engine monitoring, and (4) flight parameter recording. The first three functions are used to perform maintenance actions. The binary file *.RDF resides on the server. A binary to ASCII converter program was written in “C sharp language.” This program converts the binary flight parameters into ASCII and loads the data in an Oracle database.

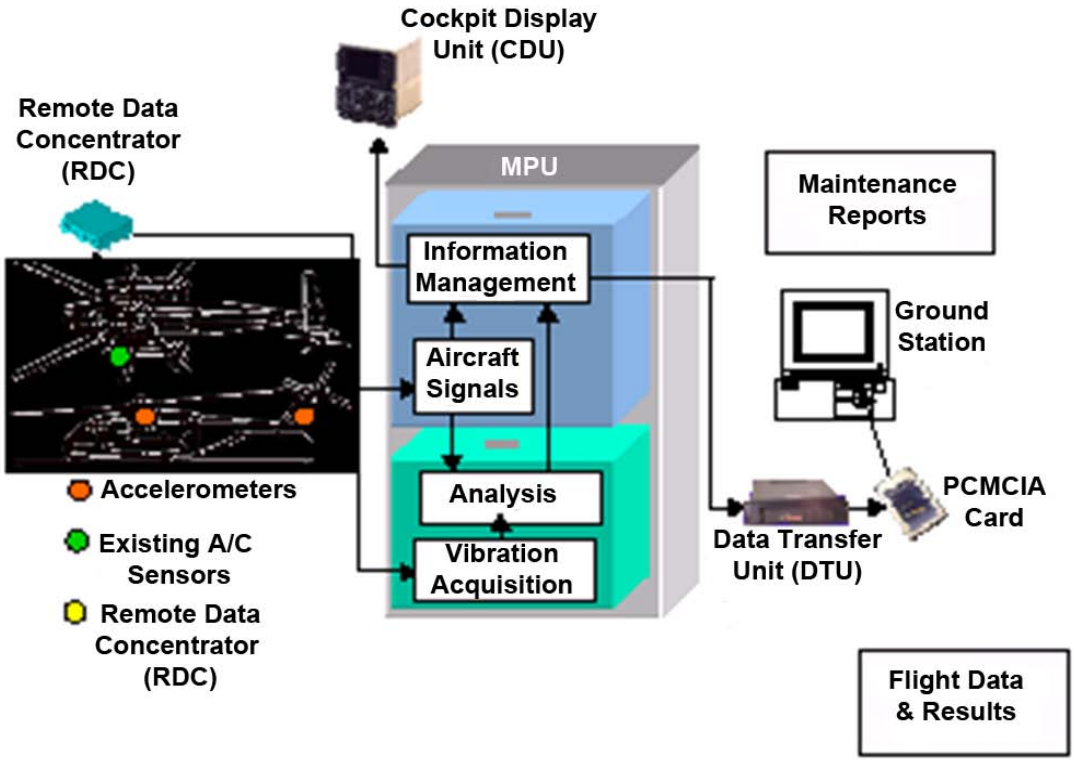

Figure 1: H-60 IMD-HUMS airborne unit and ground station

The flight parameters required for regime recognition program are Quality Controlled (QC) for valid ranges, spikes, constant values throughout the flight. The summary flight parameters QC status is written to files and the database for further investigation. The weight-on-wheel to weight-off-wheel bounce was corrected to assure the aircraft was on the ground at least two seconds continuously and in flight for more than 10 seconds. The software was developed to write flight parameter time history input files for the regime recognition program. While writing the input files, invalid parameters are corrected and interpolated. If Nz and roll are constant throughout a flight, the flight is discarded. The program recognizes approximately 315 regimes at various velocities, bank angle, Nz, rate climb/descent, power levels, and computes GW. The RR algorithm and its validation are described in References 4-5. The GW and C.G. computation approach is documented in Reference 6. The U.S. Navy usage monitoring systems on AH-1W, H-46, H-60, H-53, and V-22s are described in References 1-3 and 7-13. The approach to develop usage spectrum using regime recognition data is described in References 3, and 13-15. The usage variation modeling is suggested in Reference 16. The serial number dynamic tracking system developments are described in References 7, 12, 17, and 18. The evaluation of reliability with measured loads, usage and strength is provided in Reference 19. A model to compute cost saving with usage monitoring for the return on investment can be found in Reference 8.

3.0 Droop Stop Pounding Regime Recognition Algorithm

The H-60 rotor hub assembly consists of rotor shaft, rotor shaft extender, main rotor hub, damper, spindle, bifilar vibration absorber, swashplate, rotating scissors, and pitch control rod and are shown in Figure 2. The droop stop and flap restrainers are installed on the spindle to prevent extremely high and low blade flapping and are shown in Figure 3. With an increase in rotor rpm to 70%, the droop stop moves from its static position to dynamic. The audible knocking of droop stop during engagement or rotor stop is an indication of droop stop pounding to the pilot. The rotor blade flapping motion is responsible for droop stop pounding or mast bumping. To recognize droop pounding in a regime it is necessary to study flap motion.

The blade flap motion can be represented by infinite Fourier series (References 20-21):

$$\beta = a0 - a1s\cos\psi - b_{1s}\sin\psi - a_{2s}\cos 2\psi - b_{2s}\sin 2\psi + \ldots$$

β = flap angle (between the control axis and blade)

a_0 = coning angle

ψ = azimuth angle (is measured from downwind position in direction of rotation)

The values of a_{2s} and b_{2s} are small magnitudes and can be neglected (Reference 20). This reduces the flap motion to:

$$\beta = a0 - a1s\cos\psi - b1s\sin\psi$$

$$\beta = a0 +/- \beta 1$$

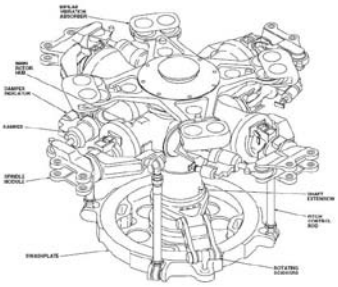

Figure 2: H-60 dynamic component assembly

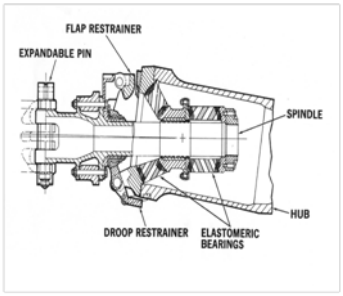

Figure 3: MH-60 flap and droop stop restrainer

The positive values of flap angle are limited by the flap restrainer shown in Figure 3 of H-60 rotor hub and spindle assembly. The negative values of flap angle are restricted by the droop restrainer. The maximum blade flap angle during a 2.0g pullout is 15 deg and minimum blade flap angle during droop stop is -8.3 deg., as shown in Figure 4. Thus droop stop pounding occurs at flap angle β <-8.5 degrees or around it.

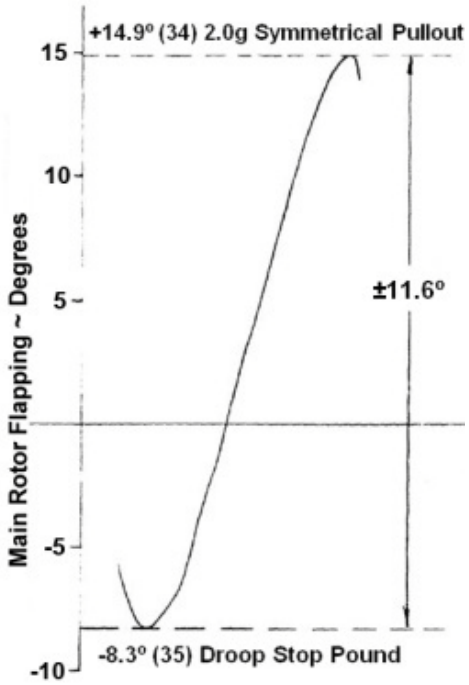

Figure 4: Flap angle requirement for droop stop pounding

The flight test data of DSP prone maneuvers: low g pushovers, rolling landings, slope landings, rotor start-stops, taxi and taxi turns was researched for rotor blade flap angle, control stick positions, rotor RPM, and vertical accelerations variations to develop a DSP recognition algorithm.

The change in collective control positions and associated low g maneuvers during 11 low g pushover maneuvers are shown in Figure 5. For the same pushover maneuvers the minimum flap angle variation with associated vertical acceleration as shown in Figure 5. The flap angle below -8.5 degree is likely to be responsible for DSP or mast bumping during pushover depending upon the flap magnitude. From Figure 6 it can be inferred that DSP is likely to occur below 0.1g during pushover as flap angle becomes less than threshold at -8.5 degree. However, for the algorithm to be conservative, threshold was set at 0.15g.

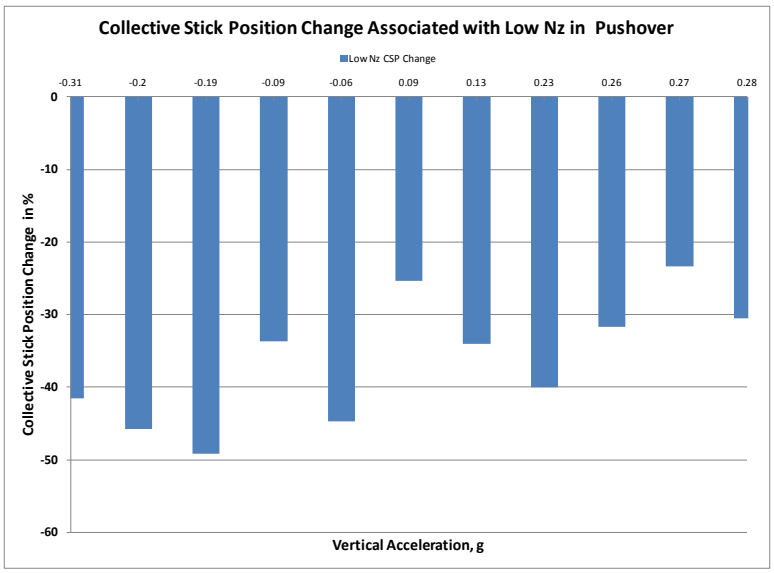

Figure 5: Collective stick position variation with vertical load factor

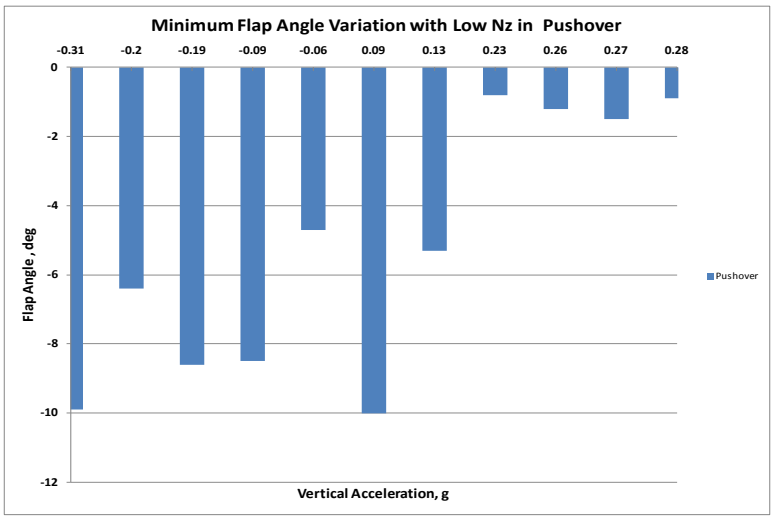

Figure 6: Flap angle variation with vertical load factor

The variation of minimum blade flap angle with lateral stick position change for 11 rolling and slope landings are shown in Figure 6. The lateral control stick position change less than -7.5% results in -9 degree rotor blade flap deflection. This threshold was utilized to recognize DSP during rolling landings. The flight test data for taxi with significant negative blade flap deflection measurement was available for only one event. The minimum blade flap deflection was not significant. Thus lateral control stick position change with low collective constraint was utilized to recognize DSP. The DSP recognition threshold selected was similar to rolling landings and is conservative.

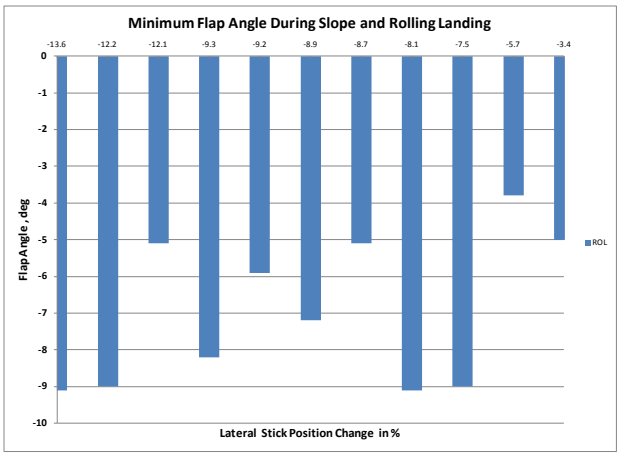

Figure 7: Minimum flap angle during slope and rolling landing and associated lateral control stick position change (%)

The variation of minimum blade flap angle with rotor RPM and lateral control position change is shown in Figure 8 for 4 rotor start and stop events. For -12.1% lateral stick position change, blade flap deflection angle was -10.0 degree with rotor RPM less than 40%. For the event with lateral stick position change of -12.8%, the blade flap deflection angle was -14 degree and rotor RPM was less than 46 %. For the other two events, blade flap deflection was less than 2 degrees. This variation was utilized to derive DSP recognition with lateral control stick position change and a constraint on collective stick position during rotor start and stop. To be conservative, the rotor RPM threshold was set at 70%, lateral control position change at -7.5%, and collective stick position less than 10%.

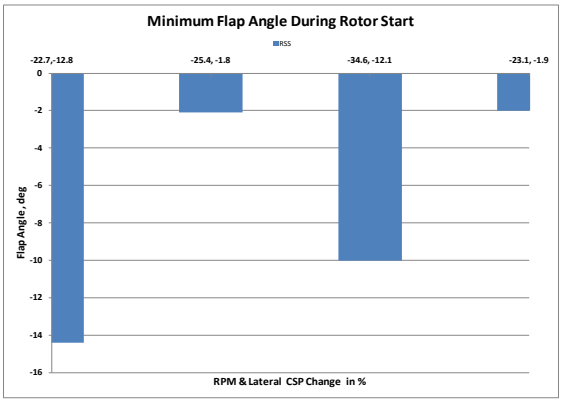

Figure 8: Minimum flap angle during rotor start and stop and associated lateral control stick position change (%)

4.0 Droop Stop Pounding Occurrences in MH-60 Fleet

DSP recognition logic was programmed and run through 58,348 flights consisting 84,549 rotor hours from 308 MH-60 IMD rotorcraft to obtain DSP utilization and regime utilization of regimes in MH-60 usage spectrum. The MH-60 IMD data regime recognition summary is shown in Table 1. The program recognizes 99.57% data, thus exceeds expectations of U.S. Army Aviation Engineering Directorate (AED), Condition Based Maintenance System for U.S. Army Aircraft, requirements, Reference 22.

Table 1: MH-60R and MH-60S regime recognition data summary

	Apr-14
MH-60 Rotorcraft equipped with IMD	308
Rotor hours (from rotor start to rotor stop)	84549
Number of flights/Files	58348
RR Recognized data (%)	99.57
Unrecognized (%)	0.43
MH-60 Rotorcraft with rotor hours > 200	152
Rotor hours for 108 rotorcraft	72121
MR-60R Rotorcraft with rotor hours > 200	89
Rotor hours for 51/89 rotorcraft	40065
MH-60 Rotorcraft with rotor hours > 200	63
Rotor hours for 57 /63 rotorcraft	32055

The DSP occurrences during rotor start and stop, taxi, taxi turns, rolling landings and pushovers are shown in Figures 9 though 13 for each rotorcraft with DSP. The wide variation in DSP usage was observed from rotorcraft to rotorcraft. The rotorcraft without DSP occurrences are not shown in Figures 9-13. The fleet occurrences of DSP during these maneuvers are significantly lower than design. The mean, mean+3s, and maximum DSP occurrences are compared with design in Table 2. For computation of DSP mean and standard deviation, rotorcraft with rotor hours greater than 200 were considered according to Reference 14. The helicopters with rotor hours greater than 200 but no DSP occurrences were not included in this statistical analysis. The average occurrences are 0.3, 0.9, 1.1, 1.2, and 3.2 for rolling landings, rotor start and stop, taxi turn, pushover, taxi respectively. The total average DSP occurrences are 7 and mean+3s are 27 and maximum 39 per 100 per compared to 100 for design. Thus the 100 DSP assumed occurrences need to be reviewed in context of 84,549 rotor hours from 308 MH-60 IMD rotorcraft. The impact of DSP occurrences during rotor start and stop, taxi, taxi turns, rolling landing on main rotor spindle fatigue damage is discussed in following paragraphs.

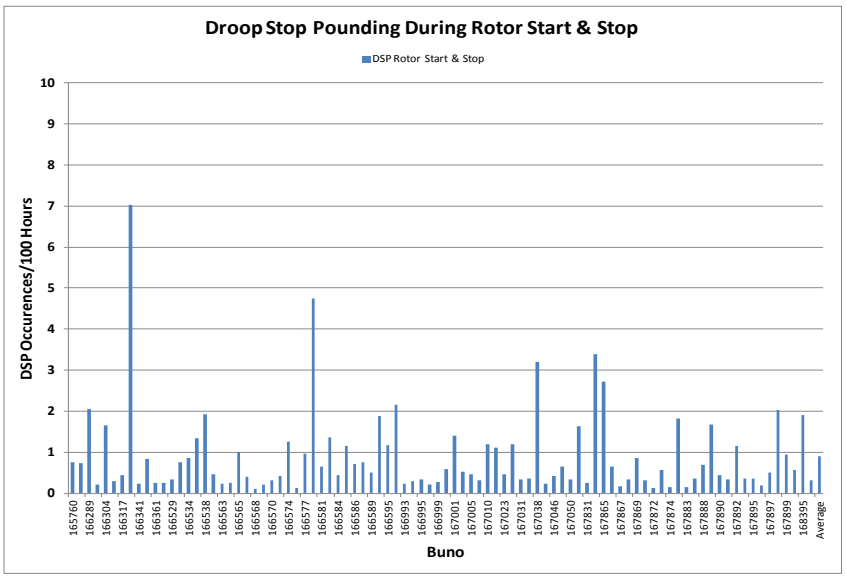

Figure 9: Individual rotorcraft DSP occurrences/ 100 hours during rotor start and stop

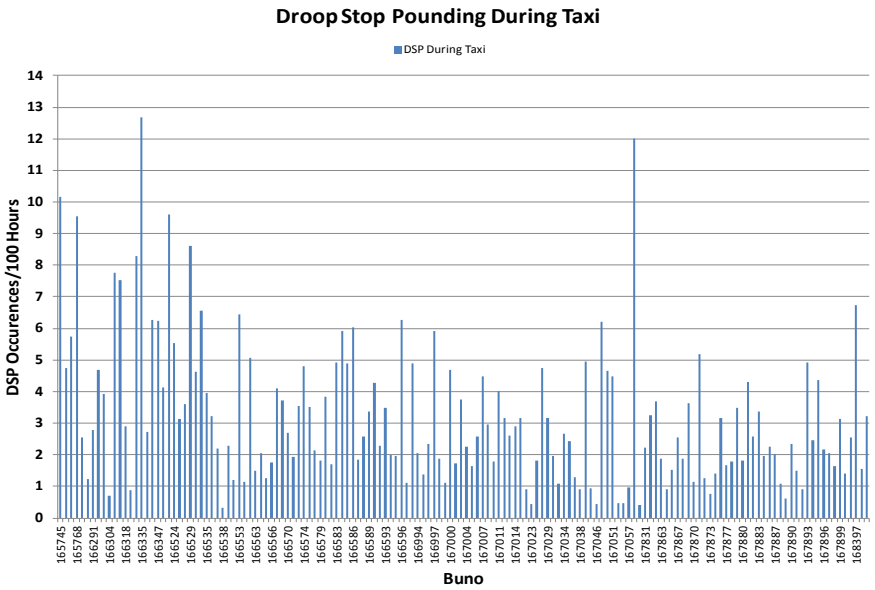

Figure 10: Individual rotorcraft DSP occurrences/ 100 hours during taxi

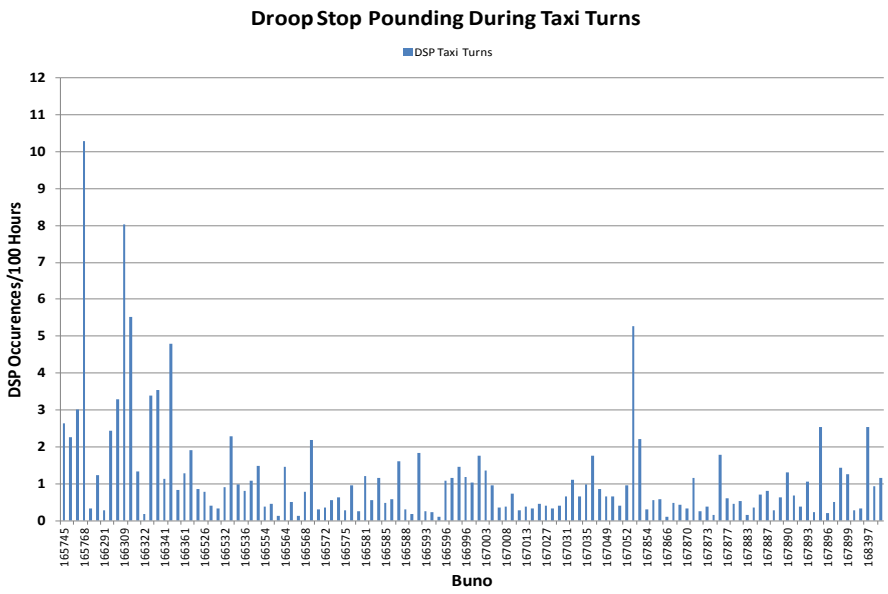

Figure 11: Individual rotorcraft DSP occurrences/ 100 hours during taxi turns

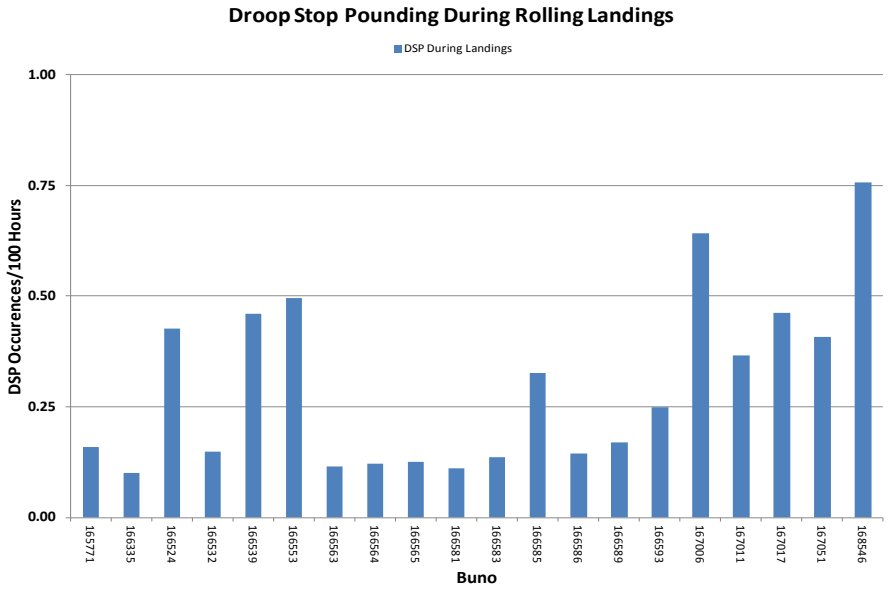

Figure 12: Individual rotorcraft DSP occurrences/ 100 hours during rolling landings

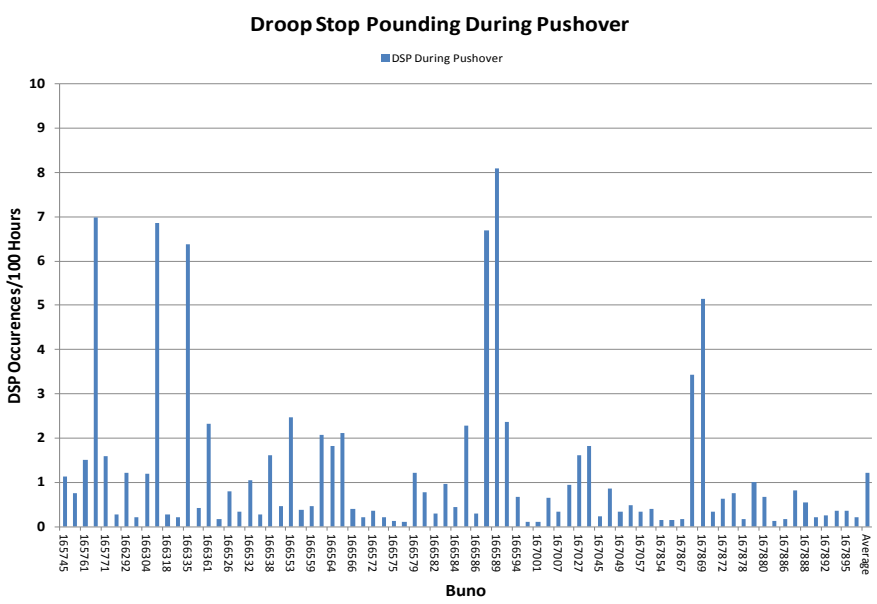

Figure 13: Individual rotorcraft DSP occurrences/ 100 hours during pushover

Table 2: DSP maneuver utilization from MH-60

Droop Stop Pounding Maneuvers Utilization from MH-60

Droop Stop Pounding Maneuvers	Design	Mean	Mean+3S	Max
Rotor Start & Stop	18	0.9	4.0	7.0
Taxi	38	3.2	10.1	12.7
Taxi Turn	34	1.1	5.5	10.3
Rolling Landings	9	0.3	0.9	0.8
Pushover	0	1.2	6.5	8.1
Total	**100**	**7**	**27**	**39**

5.0 DSP Fatigue Damage Computation

Droop Stop Pounding (DSP) causes fatigue damage to the H-60 main rotor spindle, main rotor shaft, main rotor shaft extender, main rotor hub, main gearbox, and main rotor hold hinge. The percentages of DSP fatigue damage contribution for these components are shown in Figure 14. The DSP alone causes 52% of fatigue damage to spindle and is the highest of all other components. The next most fatigue damaging regime is Ground-Air-Ground (GAG) cycle and its contribution to various components are also shown in Figure 14. The DSP and GAG together causes almost 70% fatigue damage to spindle and main rotor hub. Spindle fatigue damage sensitivity is conducted in the following section as DSP alone contributes 52% of fatigue damage.

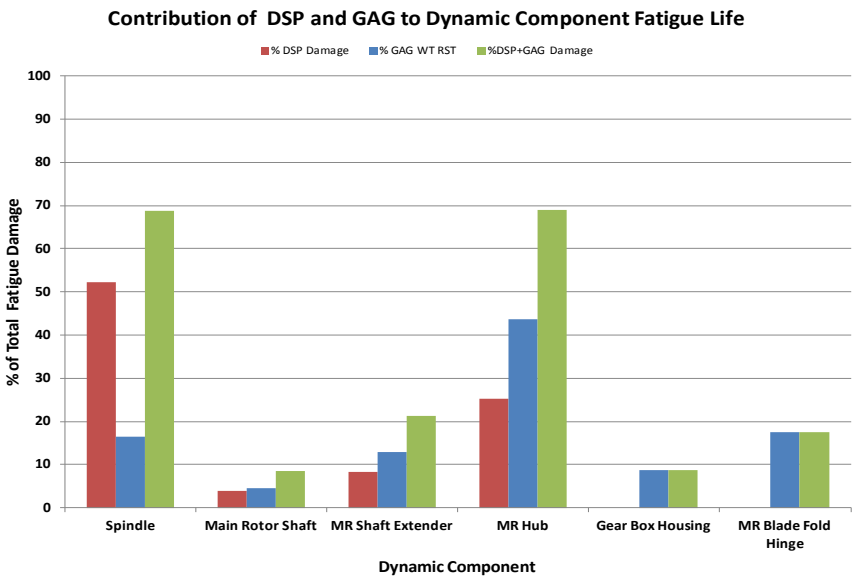

Figure 14: Contribution of DSP and GAG cycles to dynamic component fatigue life

5.1 Spindle Fatigue Damage Due to DSP

MH-60S spindle is subjected to loads/stresses as DSP occurs. There are five critical locations/failures modes of the spindle: 1) Spindle fold hinge attachment lug failure mode, 2) Spindle lock nut failure mode, 3) Spindle inboard thread failure mode, 4) Droop stop outboard cone mode, and 5) Droop stop ring failure mode. The minimum life is observed for droop stop ring failure mode shown in Figure 15.

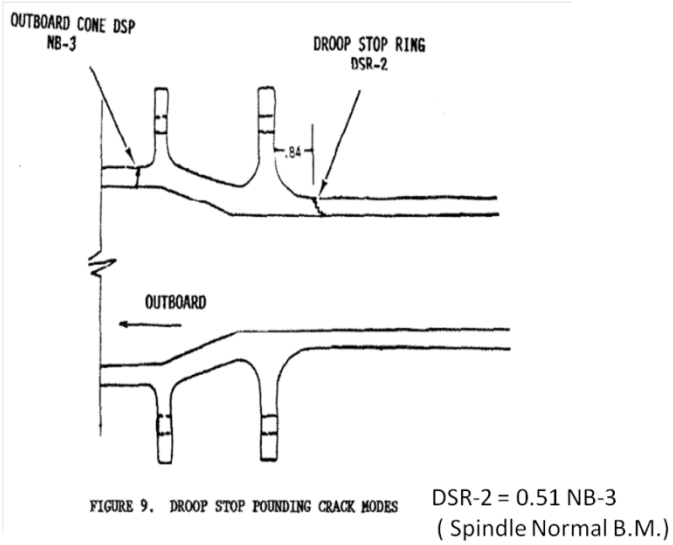

Figure 15: Spindle critical location due to droop stop pounding

Vibratory droop shank stress, DRS-2 for MH-60S is calculated using the relationship between SH-60B DSR-2 and spindle normal bending MRSNB3. The stresses at DSR-2 for rolling landing, taxi, taxi turns, and rotor start-stop are shown in Table 3. The maximum DSR-2 stress is associated with severe DSP, mean DSR-2 stress corresponds to moderate DSP and mean-1s DRS-2 stress is associated with mild DSP. From this information the standard deviation of stress is derived for each DSP prorated maneuver and is indicated in Table 3.

Table 3: DSP stresses at DSR-2 in various maneuvers

Droop Stop Pounding (DSP) Stresses at DSR2 in Various Maneuvers

	Rolling Landing	Taxi (Start-Stop)	Taxi Turns	Rotor Start-Stop
DSP Severity	Stress, PSI	Stress, PSI	Stress, PSI	Stress, PSI
Severe (Max)	37440	29150	20000	15210
Moderate (Mean)	30810	20890	20000	10960
Mild (Mean-1S)	22580	15250	20000	5000
Standard Dev	8230	5640	0	5960
Mean+1s	39040	26530	20000	16920

The DSP severity depends on the blade flapping angle amplitude reached during the DSP occurrence. The DSP stress as a function of blade flapping angle amplitude is shown in Figure 16. The regression fit to the data indicates that an increase in blade flap angle amplitude results in higher stress amplitude. The blade flapping amplitude below 10 degrees will result in stress corresponding to mild DSP severity, as shown Figure 16. The 10 degree blade flapping amplitude is just above the absolute threshold required for DSP. As blade flap amplitude increases above 10 degrees but below 12 degrees, the stress amplitude is in moderate DSP severity range whereas blade flapping amplitude above 12 degrees corresponds to severe DSP stress amplitude. From the DSP recognition developed earlier it can be seen that constrain on collective control stick and higher change in lateral control stick position results in an increased blade flap amplitude. The usage analysis reveals that magnitude of lateral control stick change is significantly lower than the change required to severe or even moderate DSP for DSP prone maneuvers: rolling landing, taxi, rotor start and stop.

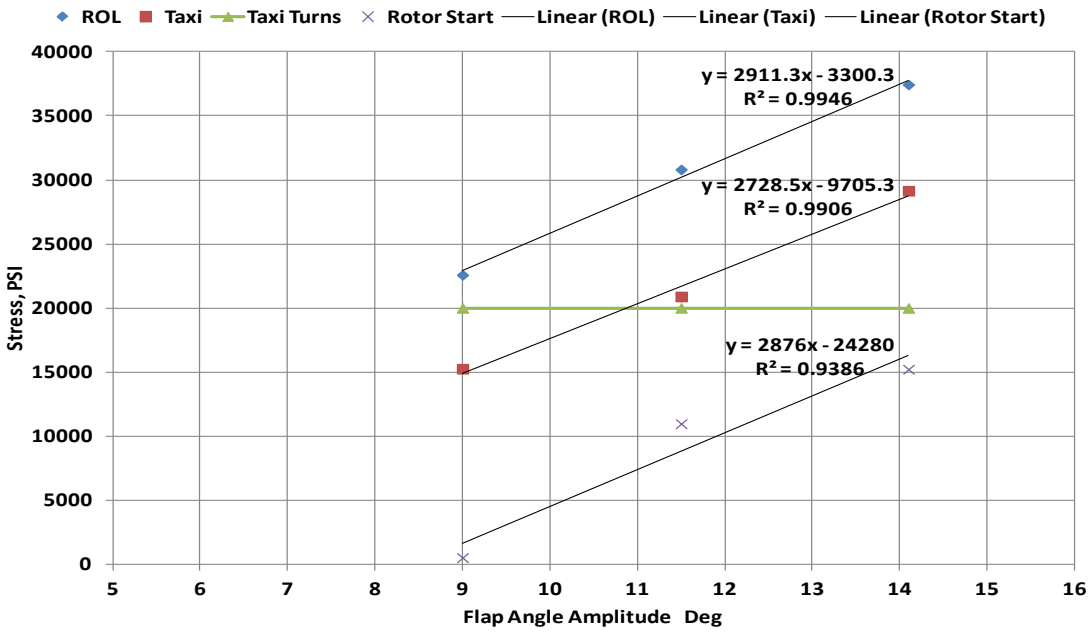

Figure 16: DSP DRS-2 stress variation with blade flap angle

The MH-60S design usage spectrum has 100 DSP occurrences per 100 hours. It has 9.91 DSP occurrences during rolling landings, 53.89 occurrences during taxi, and 36.2 occurrences during rotor start and stop. The event duration of DSP occurrence is 2 seconds resulting in total DSP time to be 200 seconds. With rotor frequency of 4.3 Hz, it will accumulate 860 DSP cycles. The DSP occurrences in DSP prone maneuvers is shown Table 2. The DSP fatigue damage computation prorate 1 displayed in Table 4 is conducted independently using the % time utilization, stresses and S-N curve. The computed fatigue damage fraction matches the one reported in MH-60S SER # 521877.

Table 4: DSP prorated fatigue damage computation

Droop Stop Pounding Prorated Fatigue Damage Computation							
Maneuver	Severity	Fraction time	Time sec	Rotor Cycles	Stress, PSI	Failure Cycles in Million	Fatigue Damage
Rolling Landing	Severe	0.0047	0.94	4	37440	0.0070	0.000577
Rolling Landing	Moderate	0.0244	4.88	21	30810	0.0160	0.001312
Taxi	Severe	0.0129	2.58	11	29150	0.0200	0.000555
Rolling Landing	Mild	0.0700	14.00	60	22580	0.0720	0.000836
Taxi	Moderate	0.3250	65.00	280	20890	0.1120	0.002496
Taxi	Mild	0.2010	40.20	173	15250	1.0890	0.000159
Rotor Start-Stop	Moderate	0.3620	72.40	311	10960	infinite	
							0.005934

The MH-60 IMD mean, mean+3s and maximum DSP occurrences are provided in Table 2. The maximum recognized prorated 33 DSP occurrences per 100 hours are considered for spindle fatigue damage assessment. Pushover DSPs are not considered

for damage assessment in the design spectrum thus are also excluded in this assessment. The recognized DSP occurrences during rolling landings, taxi, taxi turn and rotor start and stop are further prorated as severe, moderate, and mild as indicated in Table 5. The event duration of DSP occurrence is assumed to be 2 seconds resulting in total DSP time to be 66 seconds. With rotor frequency of 4.3 Hz, it will accumulate 285 cycles droop stop pounding cycles. The DSP fatigue damage computation for recognized occurrences is shown in Table 5 and is almost 50% (0.003040) compared to design (0.005934).

Table 5: DSP prorated fatigue damage computation using fleet utilization

Droop Stop Pounding Prorated Fatigue Damage Computation Using Fleet Utilization							
Maneuver	**Severity**	**Occurrences**	**Time sec**	**Rotor Cycles**	**Stress, PSI**	**Failure Cycles in Million**	**Fatigue Damage**
Rolling Landing	Severe	1	2.00	9	37440	0.0070	0.001229
Rolling Landing	Moderate	1	2.00	9	30810	0.0160	0.000538
Taxi	Severe	1	2.00	9	29150	0.0200	0.000430
Rolling Landing	Mild	1	2.00	9	22580	0.0720	0.000119
Taxi	Moderate	8	16.00	69	20890	0.1120	0.000614
Taxi	Mild	14	28.00	120	15250	1.0890	0.000111
Rotor Start-Stop	Moderate	7	14.00	60	10960	infinite	
		33.0					0.003040

5.2 Spindle Fatigue Damage for Distributed Stresses

The severe DSP corresponds to maximum stress level, moderate is equal to mean (50 percentile) and mild DSP is associated with mean-1s (16 percentile) stress levels. The mean stress level and standard deviation are utilized to construct normal cumulative probability of stress level exceedances as shown in Figure 18. Previously, three stress levels severe (maximum), moderate (50 percentile) and, mild (16 percentile) were utilized to compute DSP fatigue damage with their prorate, as shown in Tables 4 and 5. With DSP stress distributions during rotor start-stop, taxi and rolling landings refined stress prorating in many levels is possible compared to design of 3 levels. Thus seven level stress prorating corresponds to mean+1.5s, mean+1s, mean+0.5s, mean, m-0.5s, mean-1s and mean-1.5s as shown in Table 6. The design 81 DSP rotor cycles in rolling landing, 330 DSP rotor cycles in taxi, 292 DSP rotor cycles in taxi turns and 157 DSP rotor cycles in rotor start-stop were prorated similar to design but in seven levels as shown in Table 7. With distributed load levels and associated design rotor cycles the fatigue damage was reevaluated to 0.0046 and lower than the design damage of 0.005934. Thus with distributed stresses the fatigue damage reduces by 22%.

With distributed stresses in seven levels and IMD usage the fatigue damage reduces from 0.005934 to 0.0037. Thus distributed stresses and IMD usage reduces the damage by 38%. However, distributed stress fatigue damage reduction is lower than 50% observed with IMD usage because the rolling landing severe DSP stress is lower than distributed mean+1s stress. Also, the taxi severe DSP is slightly lower than distributed mean+1.5s stress.

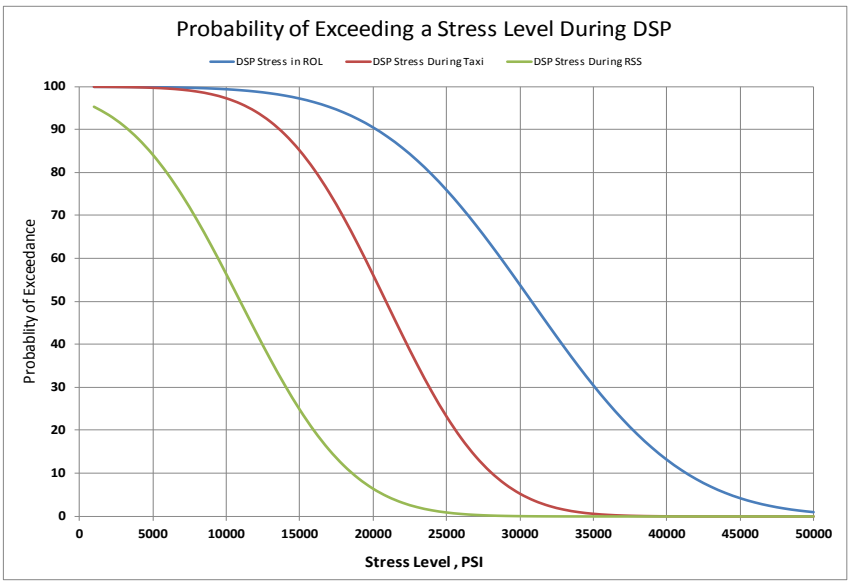

Figure 18: Probability of exceeding a stress level during DSP

Table 6: DSP distributed stresses

Droop Stop Pounding Distributed Stresses

Severity	Rolling Landing	Taxi (Start-Stop)	Taxi Turns	Rotor Start-Stop
Mean+1.5S	43155	29350	20000	19900
Mean+1S	39040	26530	20000	16920
Mean+0.5S	34925	23710	20000	13940
Mean	30810	20890	20000	10960
Mean-0.5S	26695	18070	20000	7980
Mean-1S	22580	15250	20000	5000
Mean-1.5S	18465	12430	20000	2020

Table 7: DSP distributed rotor cycles

Droop Stop Pounding Distributed Rotor cycles

Severity	Rolling Landing	Taxi (Start-Stop)	Taxi Turns	Rotor Start-Stop
Mean+1.5S	**0**	**3**	**3**	**2**
Mean+1S	**4**	**7**	**7**	**5**
Mean+0.5S	**5**	**10**	**12**	**10**
Mean	**7**	**30**	**30**	**20**
Mean-0.5S	**9**	**50**	**50**	**30**
Mean-1S	**25**	**100**	**60**	**40**
Mean-1.5S	**31**	**130**	**130**	**50**
Total	**81**	**330**	**292**	**157**

The spindle fatigue life based on design DSP occurrences, distributed DSP fatigue stresses and MH-60 IMD DSP recognized maximum occurrences is shown in Figure 19. Figure 19 clearly indicates that recognition of DSP using IMD recorded will significantly increase the fatigue life. Further spindle serial number fatigue tracking will result in cost savings.

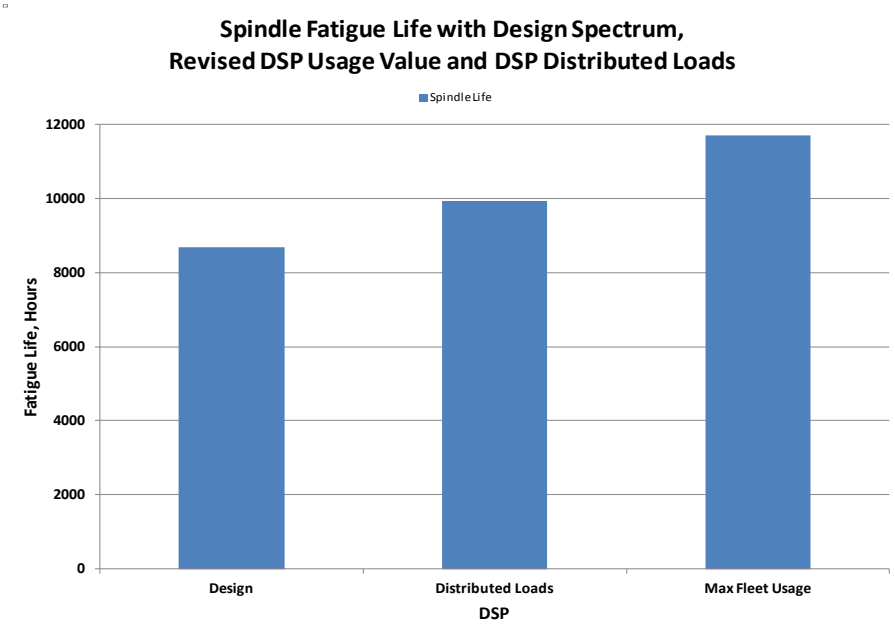

Figure 19: Spindle life (Design, Distributed DSP loads, and IMD Max. DSP Occ.)

6.0 Techniques to Reduce DSP

During rotor start and stop cyclic must be centered and collective should be raised. On rolling landing once the main wheels touchdown, the cyclic should be centered prior to reducing the collective.

7.0 Conclusions

1. The successful DSP regime recognition algorithm was developed.

2. Approximately 58,348 IMD flights consisting of 84,549 rotor hours from 308 MH-60R/S rotorcraft were analyzed using the DSP algorithm.

3. The fleet mean, mean+3s, and maximum DSP occurrences are lower than design.

4. The design DSP occurrences contribute 52% of fatigue damage to the spindle fatigue life.

5. Fleet recognized maximum DSP usage reduces the fatigue damage by 50% compared to design.

6. The DSP distributed stresses reduces the fatigue damage by 22% compared to design life for design usage. For maximum recorded usage the distributed stresses reduces fatigue damage by 38%.

7. Individual rotorcraft usage with serial number fatigue tracking will help to increase spindle fatigue life, enhance safety, and reduce cost.

8.0Acknowledgements

Authors thank Mike Stull and Mark Leonard for their significant programming and data processing contributions.

9.0 References

1. Hayden, R. and Muldoon, R., "U.S. Navy/USMC/BF Goodrich IMD COSSI Program: Status", American Helicopter Society 58th Annual National Forum Proceedings, Montreal, Canada, May 1999.

2. H-53 IMD Development Report, Air Vehicle Engineering, L-3 Communications Technical Report, 2009.

3. Thomas J, Neubert C, Little M, and Fuller B, "Implementation of Structural Health Monitoring for the USMC CH-53E", American Helicopter Society 66th Annual Forum Proceedings, Phoenix, AZ, May 11-13, 2010.

4. Moon S., and Phan, N., “Rotary Wing Aircraft Regime Recognition Algorithm Development & Validation”, American Helicopter Society 64th Annual Forum Proceedings, Montreal, Canada, May 9-11, 2008.

5. Moon S., Phan, N., and Churchill, D., “Maneuver Recognition Verification & Validation Using Visualization”, AIAC Fourteenth Australian International Aerospace Congress, 28 February 2011 through 3 March 2011.

6. Moon S., Phan, N., "Rotorcraft Gross Weight and Center of Gravity Prediction Using Regime Recognition", American Helicopter Society 67th Annual Forum Proceedings, Virginia Beach, VA, May 3-5, 2011.

7. Barndt, G. and Moon, S., “Development of a Fatigue Tracking Program for Navy Rotary Wing Aircraft”, American Helicopter Society 50th Annual National Forum Proceedings, Washington, D.C., May 1994.

8. Moon, S. and Hinger, C., “Helicopter Dynamic Components Fatigue Tracking System”, 18th ICAF Symposium, Melbourne, Australia, May 1995.

9. Augustin, M. J.,“A Review of the V-22 Health Monitoring System,” American Helicopter Society, 45th Annual National Forum Proceedings, Boston, MA, May 1989.

10. Martin, W., Collingwood, G., and Barndt, G., “Structural Life Monitoring of the V-22 Fatigue,” American Helicopter Society 55th Annual National Forum Proceedings, Montreal, Canada, May 1999.

11. Moon, S., Claus, J., Miller, C., Stull, M. and, Belville, R., “V-22 Individual Aircraft Fatigue Tracking,” International Power Lift Conference, Royal Aeronautical Society, London, UK, July 22-24, 2008.

12. MH-60S/R Condition Based Component Replacement/Retirement, Air Vehicle Engineering, Engility Corporation, Lexington Park, MD, Presentation August 14, 2012

13. MH-60R & MH-60S Usage Spectrum Development Using RR Information, Air Vehicle Engineering, Engility Corporation, Lexington Park, MD, TR 2014/01

14. Moon, S., and Simmerman, C., “The Art of Helicopter Usage Spectrum Development”, The Journal of American Helicopter Society (AHS), Vol. 53, (1), January 2008, pp. 68-86 or AHS Forum 61 Proceedings, Grapevine, Texas June 1-3, 2005.

15. Suresh Moon, Clyde Simmerman and Enrique Flores, VTUAV, Fire Scout Fatigue Usage Spectrum Development”, European Rotorcraft forum, Hamburg, 2009.

16. Moon S. and Phan, N., “Characterization of Rotorcraft Recorded Maneuver/Regime Usage Variability”, Sixth DSTO International Conference on Health and Usage Monitoring, Melbourne, Australia, 2009.

17. Moon S, Claus J, Miller C, Lloyd B, Belville R, Stull M, Kestel S, Gretchen Lofberg G, Allard M, "V-22 Web Based Fatigue & Usage Monitoring System", American Helicopter Society Forum 66 Proceedings, May 11-133, 2010, Arizona

18. H-53 SAFE Development (Usage Spectrum Development and Component Serial # Fatigue Life Expended (FLE) Computations) NAVAIR 4.3.3 & Air Vehicle Engineering L-3 Communications, Presentation, July 2, 2011

19. Moon, S., Menon, D., and Barndt G., “Fatigue Life Reliability Based on Measured Usage, Flight Loads and Fatigue Strength Variations,” The Journal of American Helicopter Society (AHS), Vol. 56, 2011 or AHS 52nd Annual National Forum Proceedings, Washington, D.C., June 4-6, 1996

20. Prouty, R. W., Helicopter Performance, Stability, and Control, PWS Publisher, 1986.

21. Gessow, A. and Meyers, G., Aerodynamics of the Helicopter, College Park Press, 1985.

22. U.S. Army Aviation Engineering Directorate (AED), Condition Based Maintenance System for U.S. Army Aircraft, 2013, ADS-79D-HDBK, Appendix B.